Study on the fatigue crack growth behavior of 30CrMnSiA Straight Attachment Lugs

LiMing Wu[1], YuTing He[1,*], HaiWei Zhang[1], Teng Zhang[1], Qing Shao[1]

[1] Aeronautics and Astronautics Engineering College, Air Force Engineering University, 710038, China
* Corresponding author: hyt666@tom.com

Abstract The finite element model of straight attachment lug subjected to axial or oblique loading is built by using finite element software, a cosine pin-bearing pressure distribution is applied on the pin-hole squeeze surface as a boundary condition. The stress intensity factor (SIF) expressions for single through-the-thickness crack in straight attachment lug that subjected to axial or oblique pin-load less than 45 degrees are determined and validated. The fatigue crack growth rate da/dN and the stress intensity factor range ΔK are obtained by using the fatigue crack growth test data and the SIF expressions. The fatigue crack growth model of the typical straight lugs is established by using the Paris law, offering an analytical as well as experimental method for assessing and designing damage tolerant attachment lugs.

Keywords attachment lug, finite element method, fatigue crack growth, stress intensity factor, the Paris law

1. Introduction

Attachment lugs are one of the most fatigue-and fracture-critical components in modern engineering structures[1]. In aircraft structures, lug-type joints are frequently used to connect major structural components or in linkage structure, theirs failure can result in disastrous accidents. In the study of fatigue crack growth and fracture behavior of attachment lugs, an accurate calculation of the stress intensity factor is essential. There are a number of different methods for determining SIF, K, for crack in aircraft attachment lug.

Over the years, several extensive studies have been made on lug fatigue performance, involving both experimental and analytical means. Liu and Kan[2] and Kirkby and Rooke[3] used the simple compounded solution method which involves superimposing known solutions, such as in Reference [4] to estimate the stress intensity factors. Schijve and Hoeymakers[5] and Wanhill[6] derived empirical K-solutions from the growth rate data for through cracks under constant amplitude loading using a backtracking method such as that proposed by James and Anderson[7]. Pian, et al[8], used the hybrid finite element method to compute the K-values for cracks oriented in various angles from the axial direction of straight lugs. Aberson and Anderson[9] used a special crack-tip singularity element to compute the stress intensity factors for a crack in a nonsymmetrical aircraft lug of an engine pylon. Impellizzeri and Rich[10] modified the exact weight function derived by Bueckner[11], for an edge crack in a semi-infinite plate, to include a series of geometry correction factors. Then they computed the K-values using the weight function method. However, at the aspect of damage tolerance design and analysis, only the situation of straight lug subjected to axial pin loading can be solved. For the straight lug and symmetric tapered lug, which are subjected to axial, oblique and transverse pin loadings, there is a lack of methods for ascertaining the crack propagation characteristics and residual strength. So, it is important to develop analytical as well as experimental procedures for assessing and designing damage tolerant attachment lugs to ensure the operational safety of aircraft[12], and to calculate the stress intensity factors (SIFs) in different geometric parameters and load conditions.

Most of the researches made the assumption that the assumed or computed pin-bearing pressure distribution for an uncracked case remains unchanged even after the crack has initiated and propagated. Based on the parametric study conducted in Reference [8], it was found that, for any given crack length, the difference in the SIF computed using the uniform and cosine pin-bearing pressure distributions was as much as 30 percent. Therefore, it is salient that the correct representation of the pin-bearing pressure distribution during the crack growth process is essential to the calculation of accurate stress intensity factors.

This paper presents a systemic study of the 30CrMnSiA straight attachment lug's fatigue crack growth behavior using the finite element software ANSYS. The finite element model of the lug is established

and the effect of geometric parameters on SIF is calculated and analyzed by the finite element method (FEM) with linear elastic assumptions, as in essence, the fatigue crack growth is brittle and it is often based on Linear Elastic Fracture Mechanics (LEFM) assumption[13]. The fatigue crack growth test and residual strength test are carried out by the material test system MTS-810, the test data validate the finite element analysis and are used to determine the constants C&m of the Paris Law. The fatigue crack growth model of the typical straight lugs is established, offering an analytical as well as experimental method for assessing and designing damage tolerant attachment lugs.

2. Finite Element Modeling and Analyzing

2.1. Finite element modeling and meshing

Figure 1 shows the size of the straight lug discussed in this paper, millimeter is used as the length unit. The length of the single through-the-thickness crack is *a*. The model is meshed with PLANE 183 triangular element, the real constant for "plane stress with thickness" is set to 6.7. The elastic modulus is 200Gpa and the Poisson ratio is 0.3. The node at the crack tip is defined as a singular point and there are 12 triangular elements around it. The radius of the 1st row of elements is *a*/10. The global elements edge length is set to 2. Figure 2 & Figure 3 show the mesh result.

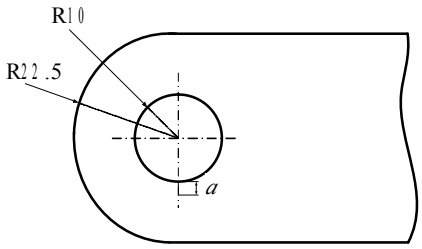

Figure 1. Size of the straight lug

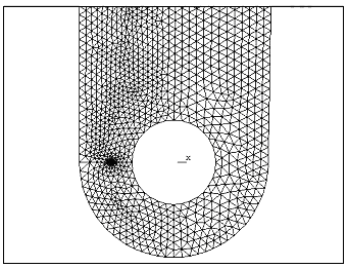
Figure 2. Mesh of the straight lug

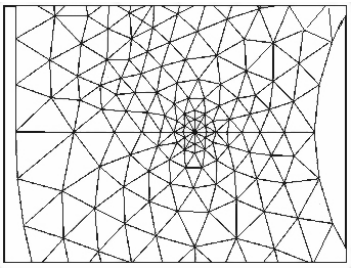
Figure 3. Mesh of the crack tip

2.2. Setting boundary conditions and applying cosine distributed load

Pin load is transferred by squeezing between the lug and the pin matched. Load and stress are supposed to keep unchangeable along the thickness of the hole. The pressure distributed on the squeeze surface follows the cosine distribution law, and the radial load P_i at the point i on the squeeze surface is equal to $P_0 \cos\gamma_i$ [14], as shown in Figure 4.

The x and y axis components of the load P_i are as follows.

$$P_{ix} = P_i \sin\gamma_i \,, \tag{1}$$

$$P_{iy} = P_i \cos\gamma_i \,. \tag{2}$$

The resultant force along y axis is shown as follow.

$$P = \sum P_{iy} = \sum P_i \cos\gamma_i = \sum P_0 \cos^2\gamma_i \,. \tag{3}$$

The cosine distributed nodal force is applied on the nodes on the surface ABC. All the nodes on the symmetry plane of the lug are selected and the displacement values are set to zero. Figure 5 shows the boundary conditions.

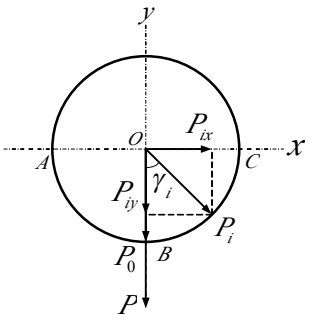

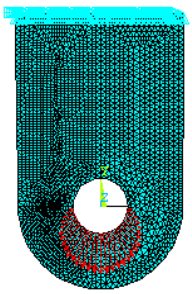

Figure 4. Pin-loading on the squeeze surface

Figure 5. Boundary conditions

2.3. Results analysis

Figure 6 and Figure7 respectively show the Von Mises stress distribution around the lug's hole and the crack tip.

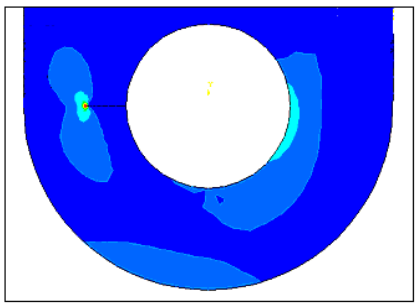

Figure 6. Stress distribution around the lug's hole

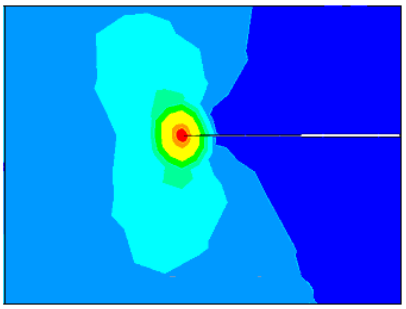

Figure 7. Stress distribution around the crack tip

SIFs of cracks with different lengths are calculated by three methods. Case 1 uses the equation that is used for estimating the straight lugs' critical load in [15] (see formula (4)) to calculate the SIFs. Case 2 uses the configuration factor J_{41L} in [15] (see Figure 8) to get the SIFs' values. This paper calculates the SIFs by finite element method, and the results are shown as case 3 in Figure 9 to compare with the other two cases.

In reference [15] (page 270), it is indicated that the critical load $[P]_c$ of the attachment lug subjected to axial pin-load is

$$[P]_C = \frac{2R_2 tK_C}{\beta\sqrt{\pi a}}. \tag{4}$$

Where

$$\beta = \left(\frac{2W}{1.971D}\beta_1 + \frac{1}{2}\beta_2\right)\cdot\beta_{fw}, \tag{5}$$

$$\beta_1 = \frac{0.31711}{\left(0.3857 + \frac{a}{R_1}\right)^{1.33734}}, \tag{6}$$

$$\beta_2 = \frac{0.8734}{0.3246 + \frac{a}{R_1}} + 0.6762, \tag{7}$$

$$\beta_{fw} = \sqrt{\sec\left(\frac{\pi}{2}\cdot\frac{2R_1 + a}{2R_2 - a}\right)}. \tag{8}$$

In reference [15] (page 139), the SIF of attachment lug subjected to axial pin-load is equal to

$$K = J_{41Z}\cdot\sigma\cdot\sqrt{\pi a}. \tag{9}$$

where the configuration factor J_{41L} can be determined by using Figure 8.

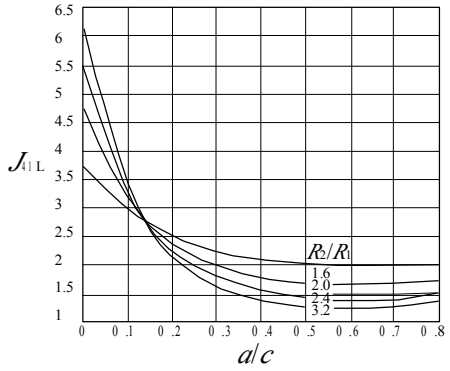

Figure 8. The configuration factor J_{41L} curves

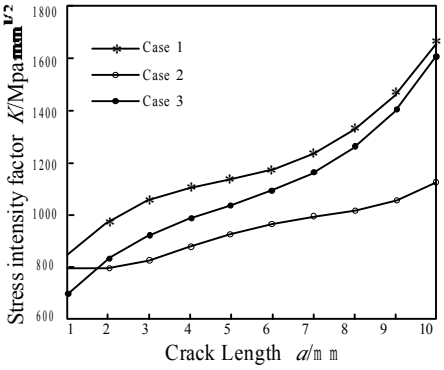

Figure 9. Comparison of the stress intensity factors

3. Calculation of the SIF equations

The geometric parameters of the lug are wrote to the APDL program text file and executed by ANSYS to solve the SIFs automatically and efficiently. The case of the straight attachment lug subjected to axial pin-load is taken as an example for illustrating the approach. Figure 10 shows the parameterized geometry of the lug.

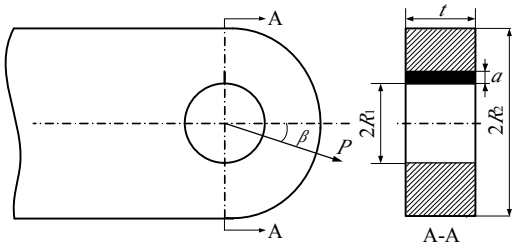

Figure 10. Geometry of the straight attachment lug

The influence law of the dimensionless crack length (a/R_1), the ratio of outer radius to inside radius (R_2/R_1) and the inside radius (R_1) on the SIF are studied, and then, the equation (4) is modified to fit the SIF equation for the straight attachment lug with a single through-the-thickness crack.

Table 1 shows the solving idea. K, K_1, K_2, K_3 stand for the SIFs calculated by equation (4) and represent the values that need to be modified by the influence law of a/R_1, R_2/R_1 and R_1 respectively. K' stands for the SIF calculated by ANSYS as the reference exact value for modifying K_1, K_2, K_3.

Table 1. Solving the SIF equation of the straight lug subjected to axial pin-load

Variate	Invariants	K	K'	$(K')_i/K_i$	Calculating process
$(a/R_1)_1$	R_2/R_1, R_1	$(K_1)_1$	$(K')_1$	$(K')_1/(K_1)_1$	$(a/R_1)_i$ is set as the variate, while $(K')_i/(K_1)_i$ as the dependent variable, function $g(a/R_1)$ can be fitted as below.
⋮	⋮	⋮	⋮	⋮	
$(a/R_1)_n$	R_2/R_1, R_1	$(K_1)_n$	$(K')_n$	$(K')_n/(K_1)_n$	$K_2=K_1\cdot g(a/R_1)$ (10)
$(R_2/R_1)_1$	a/R_1, R_1	$(K_2)_1$	$(K')_1$	$(K')_1/(K_2)_1$	$(R_2/R_1)_i$ is set as the variate, while $(K')_i/(K_2)_i$ as the dependent variable, function $f(R_2/R_1)$ can be fitted as below.
⋮	⋮	⋮	⋮	⋮	
$(R_2/R_1)_n$	a/R_1, R_1	$(K_2)_n$	$(K')_n$	$(K')_n/(K_2)_n$	$K_3=K_2\cdot f(R_2/R_1)= K_1\cdot g(a/R_1)\ f(R_2/R_1)$ (11)
$(R_1)_1$	a/R_1, R_2/R_1	$(K_3)_1$	$(K')_1$	$(K')_1/(K_3)_1$	$(R_1)_i$ is set as the variate, while $(K')_i/(K_3)_i$ as the dependent variable, function $h(R_1)$ can be fitted.
⋮	⋮	⋮	⋮	⋮	Finally the straight attachment lug's SIF equation can be obtained as below.
$(R_1)_n$	a/R_1, R_2/R_1	$(K_3)_n$	$(K')_n$	$(K')_n/(K_3)_n$	$K=K_3\cdot h(R_1)=K_1g(a/R_1)\cdot f(R_2/R_1)\cdot h(R_1)$ $=K_1\mathrm{F}(a/R_1,R_2/R_1, R_1)$ (12)

The value of a/R_1 is increased from 0.1 to 1.6 by 0.1 while the others are fixed, K_1 can be modified as $K_2=K_1*g(a/R_1)$, where

$$g(a/R_1)=-0.1285*(a/R_1)^2+0.3059*(a/R_1)+0.8228 \tag{13}$$

The value of R_2/R_1 is increased from 1.5 to 3 by 0.1 while the others are fixed, K_2 can be modified as $K_3=K_2*f(R_2/R_1)$, where

$$f(R_2/R_1)=-0.1654*(R_2/R_1)^4+1.6326*(R_2/R_1)^3-6.0293*(R_2/R_1)^2+9.9046*(R_2/R_1)-5.1399 \tag{14}$$

The value of R_1 is increased from 5 to 20 by 1 while the others are fixed, the function $h(R_1)$ can be obtained as $h(R_1)= 0.99$, it is obvious that the effect of R_1 on SIF is less than the other parameters. Finally we can obtain the modified straight attachment lug's SIF equation as $K=K_3*h(R_1)$, the SIF equation of straight lug (Figure 10) is obtained as blows.

$$K = F\cdot\sigma\cdot\sqrt{\pi\cdot a}. \tag{15}$$

Where

$$\sigma = \frac{P}{2ct}, \tag{16}$$

$$c = R_2 - R_1, \tag{17}$$

$$F = f_{ar}\cdot f_{fw}\cdot f_r, \tag{18}$$

$$f_{ar} = \frac{1.98R_2}{1.971R_1}\cdot\frac{0.31711}{\left(0.3857+\frac{a}{R_1}\right)^{1.33734}}+\frac{1}{2}\cdot\left(0.8734/\left(0.3246+a/R\right)+0.6762\right), \tag{19}$$

$$f_{fw} = \sqrt{\sec\left(\frac{\pi}{2}\cdot\frac{2R_1+a}{2R_2-a}\right)}, \tag{20}$$

$$f_r = \left(-0.1654\cdot\left(\frac{R_2}{R_1}\right)^4+1.6326\cdot\left(\frac{R_2}{R_1}\right)^3-6.0293\cdot\left(\frac{R_2}{R_1}\right)^2+9.9046\cdot\left(\frac{R_2}{R_1}\right)-5.1399\right)\cdot \tag{21}$$

Scope of application：

$$0.1\le\frac{a}{R_1}\le 1.6,\quad 1.5\le\frac{R_2}{R_1}\le 3,\quad 5\le R_1\le 20.$$

In the same way, considering the load degrees β additionally, the SIF equation of the straight attachment lugs subjected to oblique pin-load less than 45 degrees can be obtained as below.

$$K = F\cdot\sigma\cdot\sqrt{\pi\cdot a} \tag{22}$$

where

$$\sigma = \frac{P}{2ct}, \tag{23}$$

$$c = R_2 - R_1, \tag{24}$$

$$F = f_\beta\cdot f_{ar}\cdot f'_{ar}\cdot f_{fw}\cdot f_{rr}, \tag{25}$$

$$f_\beta = -3.7107\times10^{-6}\cdot\beta^3+8.4026\times10^{-5}\cdot\beta^2+0.0092469\cdot\beta+1.05, \tag{26}$$

$$f_{ar} = \frac{1.98R_2}{1.971r_1}\cdot\frac{0.31711}{\left(0.3857+a/R_1\right)^{1.33734}}+\frac{1}{2}\cdot\left(0.8734/(0.3246+a/R_1)+0.6762\right), \tag{27}$$

$$f'_{ar} = -0.063305\cdot\left(\frac{a}{R_1}\right)^2+0.067224\cdot\frac{a}{R_1}+0.94853, \tag{28}$$

$$f_{fw}=\sqrt{\sec\left(\frac{\pi}{2}\cdot\frac{2R_1+a}{2R_2-a}\right)}\ , \tag{29}$$

$$f_{rr}=\left(-0.1654\left(\frac{R_2}{R_1}\right)^4+1.6326\left(\frac{R_2}{R_1}\right)^3-6.0293\left(\frac{R_2}{R_1}\right)^2+9.9046\left(\frac{R_2}{R_1}\right)-5.1399\right)\cdot \tag{30}$$

Scope of application：

$$5°\le\beta\le45°,\ \ 0.1\le\frac{a}{R_1}\le1.6,\ \ 1.5\le\frac{R_2}{R_1}\le3,\ \ 5\le R_1\le20\ .$$

4. Fatigue crack growth test and residual strength test

4.1 Test pieces

Figure 11 shows the dimensional drawing of the straight attachment lug piece. There is a small slot made by electrical discharge machine (EDM) besides the lug hole with an angle of θ=90° or θ=60°. The slot length a_0 is approximately equal to 1mm. The lugs pieces subjected to axial (θ=90°) or 30 degrees oblique (θ=60°) pin-load are all made of 30CrMnSiA material, 4 pieces for each case.

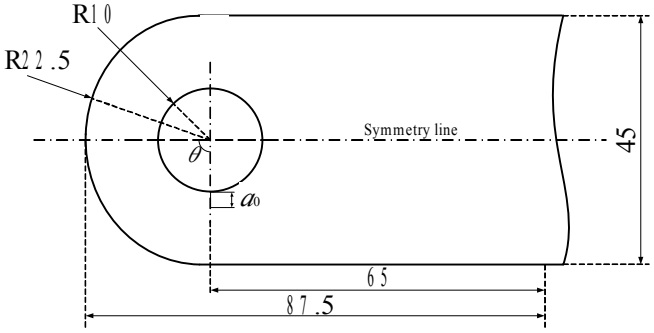

Figure 11. Geometry of the test piece

4.2 Test equipments and loading requirement

The tests are carried out on the material test system MTS-810 (load relative error <±2%) with a constant amplitude loading spectrum of sine waveform. The length of the crack is observed and measured by JXD-250mm scale microscope with a precision of 0.01mm.

Surface around test piece's wire-cutting slot tip is polished by a sand paper along the direction perpendicular to the slot direction. Peak load P_{pp} in the crack growth preparation test is 13.85KN, valley load P_{pv} is 0.83KN, R=0.06, load frequency is 5Hz. A crack with a length of 0.314mm was observed when fatigue cycle reaches about 15000, and grows to 0.612mm when 21000 cycles. The a-N data shows that the crack is growing steadily under the peak load of the fatigue crack growth test P_p=20.77KN and the valley load P_v=1.246KN.

Table 2 shows values of the test load.

Table 2. The test load values

Case	P_{pp}/(KN)	P_{pv}/ (KN)	P_p/(KN)	P_v/(KN)
θ=90°	13.85	0.83	20.77	1.25
θ=60°	13.85	0.83	20.77	1.25

4.3 Fatigue crack growth test

Figure 14 & Figure 15 show the experimental scene.

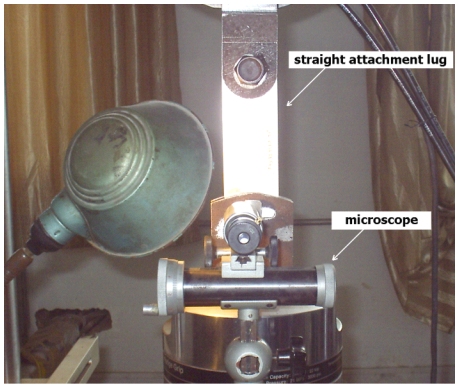

Figure 14. Experimental field of the case of θ=90°

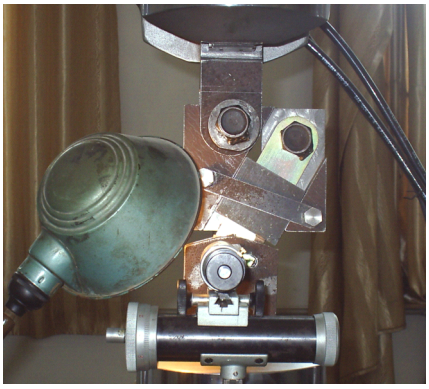
Figure 15. Experimental field of the case of θ=60°

The micro objective is aimed at the wire-cutting slot tip for detecting the fatigue crack in time. The frequency is changed to 1Hz every other 1000~2000 cycles in order to observe the crack length and record the *a*-*N* data.

4.5 Residual strength test

After obtaining enough *a*-*N* data, the test pieces with different residual fatigue crack lengths are loaded with a sustained increasing load till the test pieces fracture, the corresponding residual strength data are recorded in Table 3 & Table 4.

Table 3. The residual strength test results of the lugs subjected to axial pin-load

test piece num.	No.1	No.2	No.3	No.4
crack length *a*/(mm)	7.109	8.127	8.972	10.115
residual strength *P*/(KN)	91.456	83.242	78.051	72.947

Table 4. The residual strength test results of the lugs subjected to 30 degrees oblique pin-load

test piece num.	No.1	No.2	No.3	No.4
crack length *a*/(mm)	10.58	10.99	11.45	9.98
residual strength *P*/(KN)	58.54	42.38	40.24	58.8

The data of crack length *a* and corresponding residual strength *P* in Table 4 & Table 5 are used to substitute the *a*&*P* in formula (15) and formula(22) to calculate the SIFs. The SIFs of the axial pin-load case are: 164.30, 162.47, 166.37, 184.04, while the other case's SIFs are: 214.91, 162.08, 171.77, 179.69, the unit is $MPa\cdot\sqrt{m}$. As the fracture toughness of the material 30CrMnSiA with thickness 6.7mm is around 180 $MPa\cdot\sqrt{m}$ [16], it shows the SIFs calculated by formula (15) and formulas (22) are consistent with the true values.

5. Establishment of the fatigue crack growth model

The fatigue crack growth data are fitted by using least square method, the curves are shown in Figure16 and Figure 17.

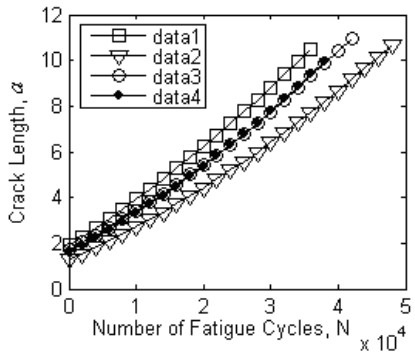

Figure 16. *a*-*N* curves of the case of axial pin-load

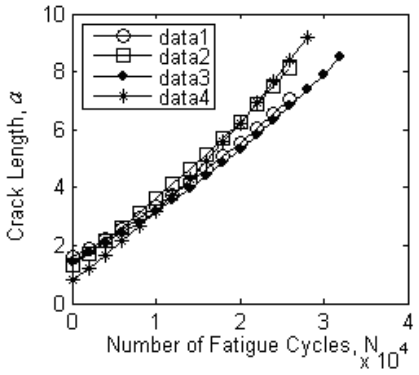

Figure 17. *a*-*N* curves of the case of 30° pin-load

The *a*-*N* data are calculated by the seven points incremental polynomial method[16]. The SIF range value ΔK and da/dN can be obtained by the fitted crack length value a^*. Table 5 shows the data processing of the test piece No.1.

Table 5. Data processing of the test piece No.1

N/(cycle)	a /(mm)	a^*/(mm)	da/dN	ΔK/(MPa·m$^{1/2}$)	lg(da/dN)	$lg(\Delta K)$
0	1.539					
2000	1.967					
4000	2.276					
6000	2.506	2.579	1.79E-7	26.556	1.424	-6.746
8000	2.958	2.927	1.85E-7	27.292	1.436	-6.732
10000	3.307	3.316	2.01E-7	28.026	1.447	-6.697
12000	3.767	3.752	2.14E-7	28.781	1.459	-6.669
14000	4.159	4.186	2.16E-7	29.497	1.469	-6.665
16000	4.652	4.629	2.24E-7	30.218	1.480	-6.649
18000	5.091	5.074	2.31E-7	30.956	1.490	-6.636
20000	5.503	5.543	2.43E-7	31.771	1.502	-6.614
21800	5.981	5.976	2.47E-7	32.577	1.512	-6.608
23000	6.291	6.278	2.59E-7	33.180	1.520	-6.585
24000	6.578					
25000	6.756					
26000	7.109					

The da/dN data of the other three test pieces can be obtained by the same method. The data points of region II are fitted by the least square method to get the lg(da/dN)~lg(ΔK) curve. Figure18 shows the fitted line of the data points.

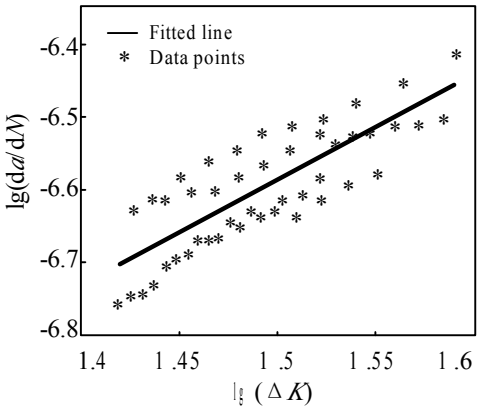

Figure 18. lg(da/dN)~lg(ΔK) curve of the axial pin-load case

The equation of the line is shown as below.

$$\lg(da/dN) = 1.4231 \cdot \lg(\Delta K) - 8.7221. \tag{31}$$

The Paris equation is

$$da/dN = C(\Delta K)^m. \tag{32}$$

In order to get the values of C and m, the paper takes the logarithm on both sides of the equation (32).

$$\lg(da/dN) = m \cdot \lg(\Delta K) + \lg C. \tag{33}$$

The values of the Paris constants C and m are obtained by comparing the equation (31) with (33).

C=1.896E-09, m=1.4231.

The lg(da/dN)~lg(ΔK) curve of region II of the lugs subjected to 30 degrees oblique pin-load can be got by the same method. Figure 19 shows the lg(da/dN)~lg(ΔK) curve.

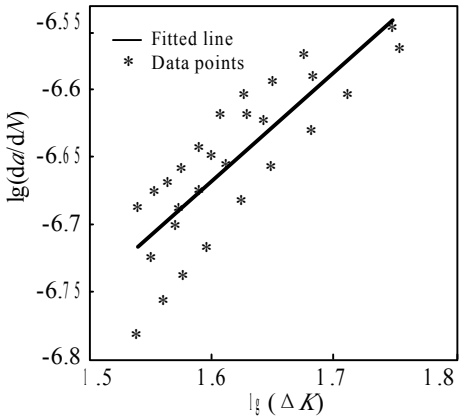

Figure 19. lg(da/dN)~lg(ΔK) curve of the 30 degrees oblique pin-load case

The equation of the line and the values of the Paris constants C and m are shown as below.

$$\lg(da/dN) = 0.7649 \cdot \lg(\Delta K) - 7.8902 \tag{34}$$

C=1.2877E-08, m=0.7649.

6. Conclusions

Analytical and experimental investigations for fatigue crack growth behavior of 30CrMnSiA straight attachment lugs were performed. From this investigation followings are concluded.

1. The boundary conditions of the finite element model is consistent with the true condition, cosine distributing load is the key of ensuring precision of FEM analysis.
2. The expressions of the SIFs of straight lugs subjected to axial or less than 45 degrees oblique pin-load are determined and validated. Based on this, the stress intensity factor range (ΔK) can be calculated.
3. The fatigue crack growth model of the typical straight lugs is established, offering an analytical as well as experimental method for assessing and designing damage tolerant attachment lugs in engineering.

References

[1] R. Rigby, M.H. Aliabadi. Stress intensity factors for cracks at attachment lugs. Eng. Failure Anal. 1997;4(2):133-146.
[2] Liu, A. F., Kan, H. P.. Test and Analysis of Cracked lugs. Frac. 1977;3: 567-664.

[3] Kirkby, W. T., and Rooke, D. P.. A Fracture Mechanics Study of Residual Strength of Pin-Lug Specimens. Frac. Mech. in Eng. Practice. 1977: 339.
[4] Cartwright, D. J., and Rooke, D. P.. Approximate Stress Intensity Factors Compounded from Known Solutions. Eng. Frac. Mech. 1974;6:563-571.
[5] Schijve, J., and Hoeymakers, A.H.W.. Fatigue Crack Growth in Lugs and the Stress Intensity Factor. Report LR-273, Delft University of Technology, Delft, the Netherlands, July 1978.
[6] Wanhill, R.J.H., and Lof, C.F.. Calculation of Stress Intensity Factors for Corner Cracking in a Lug. Frac. Mech. Design Methodology. ARGARD CP221, February 1977, Paper No. 8.
[7] James, L. A., and Anderson, W. E.. A Simple Experimental Procedure for Stress Intensity Factor Calibration. Eng. Frac. Mech. 1969;1:565-568.
[8] Pian, T. H. H., Mar, J. W., Orringer, O., and Stalk, G.. Numerical Computation of Stress Intensity Factors for Aircraft Structural Details by the Finite Element Method. AFFDL-TR-76-12, Air Force Flight Dynamics Laboratory, May 1976.
[9] Aberson, J. A., Anderson, J. M.. Cracked Finite-Elements Proposed for NASTRAN. Third NASTRAN Users' Colloquium, NASA TMX-2893, 1973:531-550.
[10] Impellizzeri, L. F., and Rich, D. L.. Spectrum Fatigue Crack Growth in Lugs. Fatigue Crack Growth Under Spectrum Loads, ASTM STP 595, 1976:320-336.
[11] Bueckner, H. F.. Weight Functions for the Notched Bar. Zeitschrift for Angewandte Mathematik und Mechanik. 1971;51: 97-109.
[12] Jong-Ho Kim, Soon-Bok Lee, Seong-Gu Hong. Fatigue crack growth behavior of Al7075-T7451 attachment lugs under flight spectrum variation. Eng. Fract. Mech. 2003;40:135-144.
[13] S.Baster, L. Molent, N.Goldsmith, R.Jones. An experimental evaluation of fatigue crack growth. Eng. Fail. Anal. 2005;12:99-128.
[14] Xue Jingchuan. Bolt and Lug Strength Analysis Handbook. Beijing: Aviation Industry Press;1998.
[15] Zheng Xiaoling. Civil Aircraft Durability and Damage Tolerance Design Handbook. Beijing: Aviation Industry Press;2003.
[16] Interpreted by Scientific and Technical Research Institute of Ministry of Aero-space Industry. USAF Damage Tolerance Design Handbook. Xi'an: Northwest Polytechnical University Press;1989.